iScience, Volume *25*

Supplemental information

Borrelia burgdorferi modulates the physical forces and immunity signaling in endothelial cells

Raúl Aparicio Yuste, Marie Muenkel, Konstantinos Axarlis, María J. Gómez Benito, Annalena Reuss, Grace Blacker, Michal Caspi Tal, Peter Kraiczy, and Effie E. Bastounis

Supplemental Figure 1

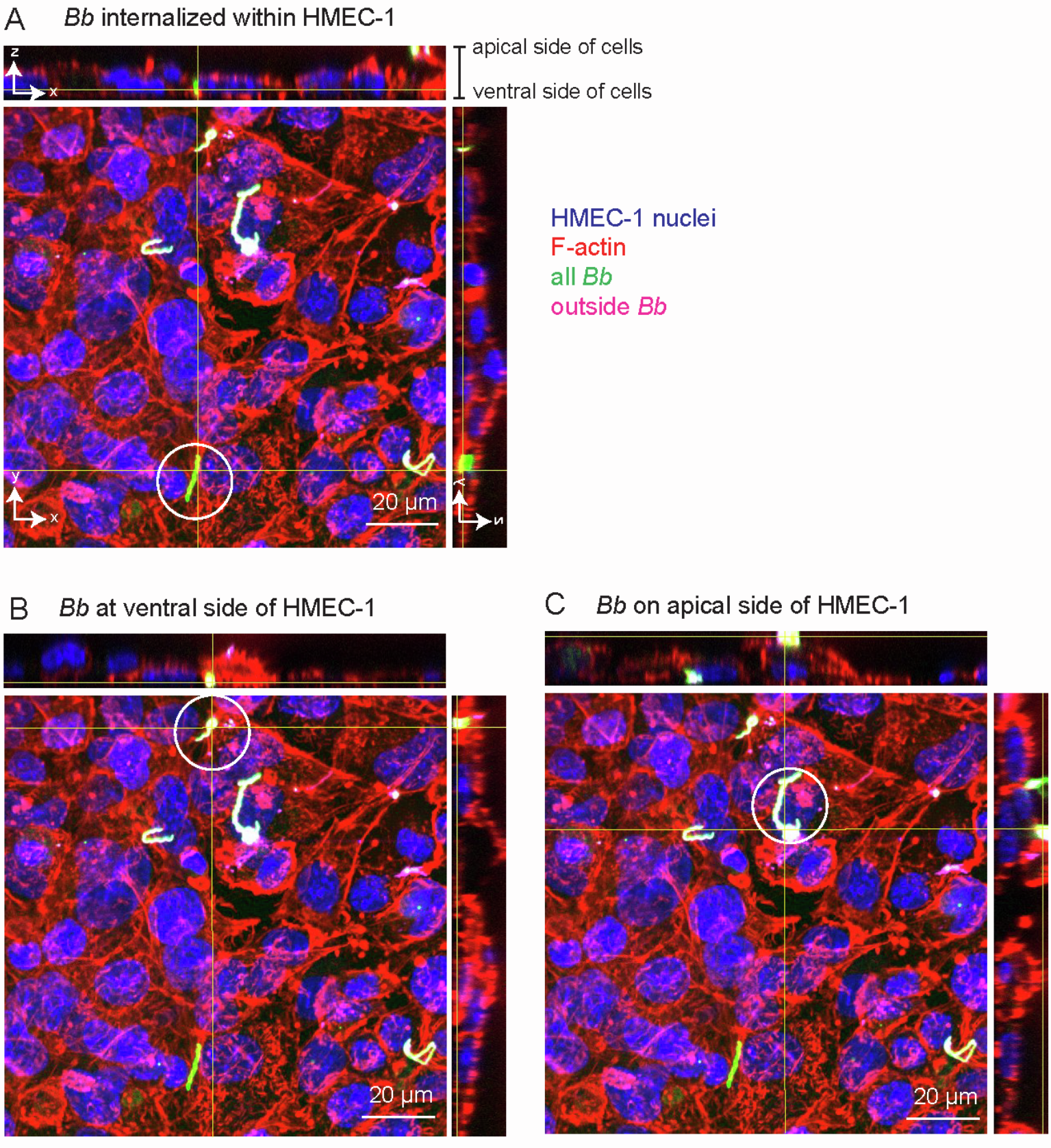

Supplemental Figure 2

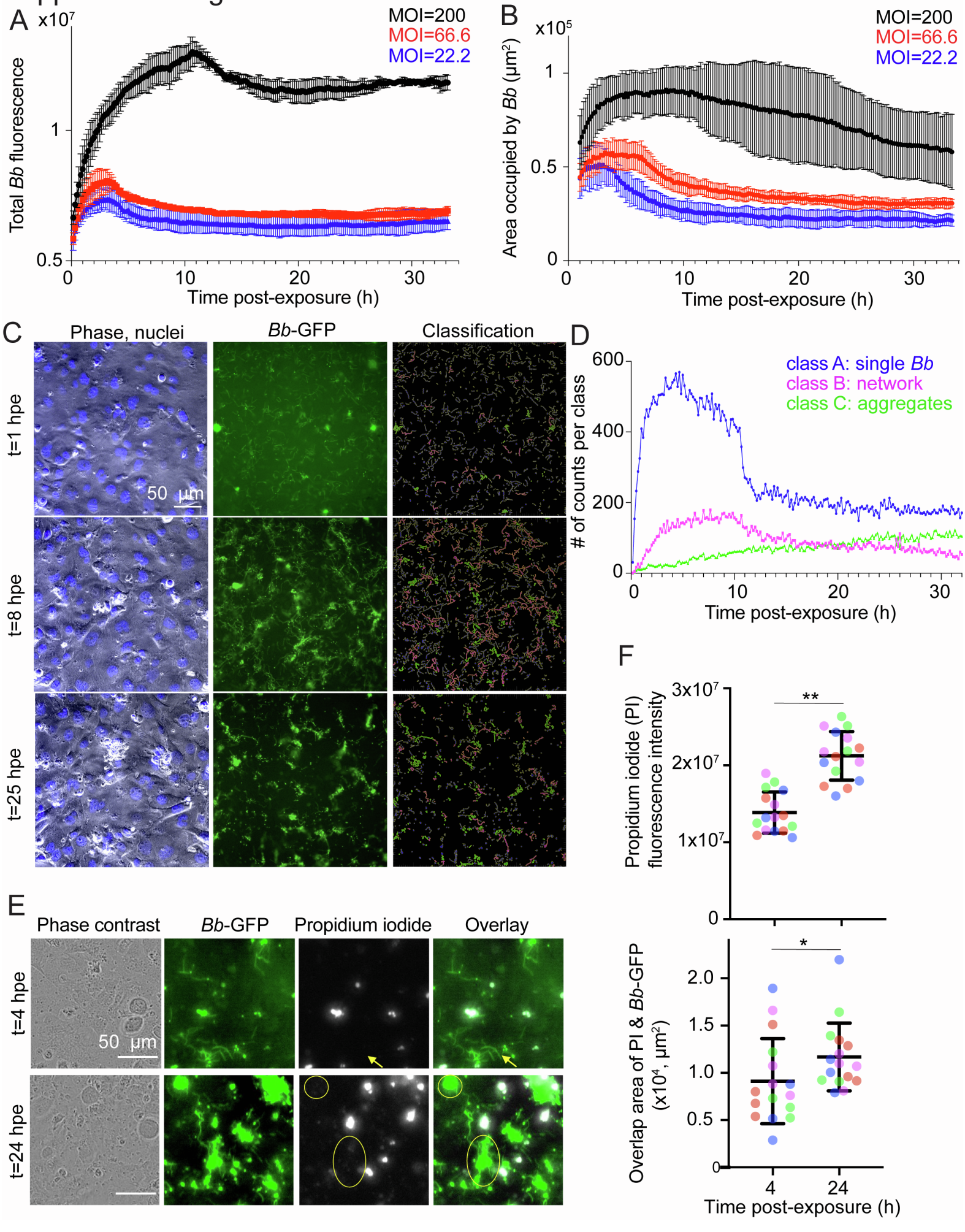

Supplemental Figure 3

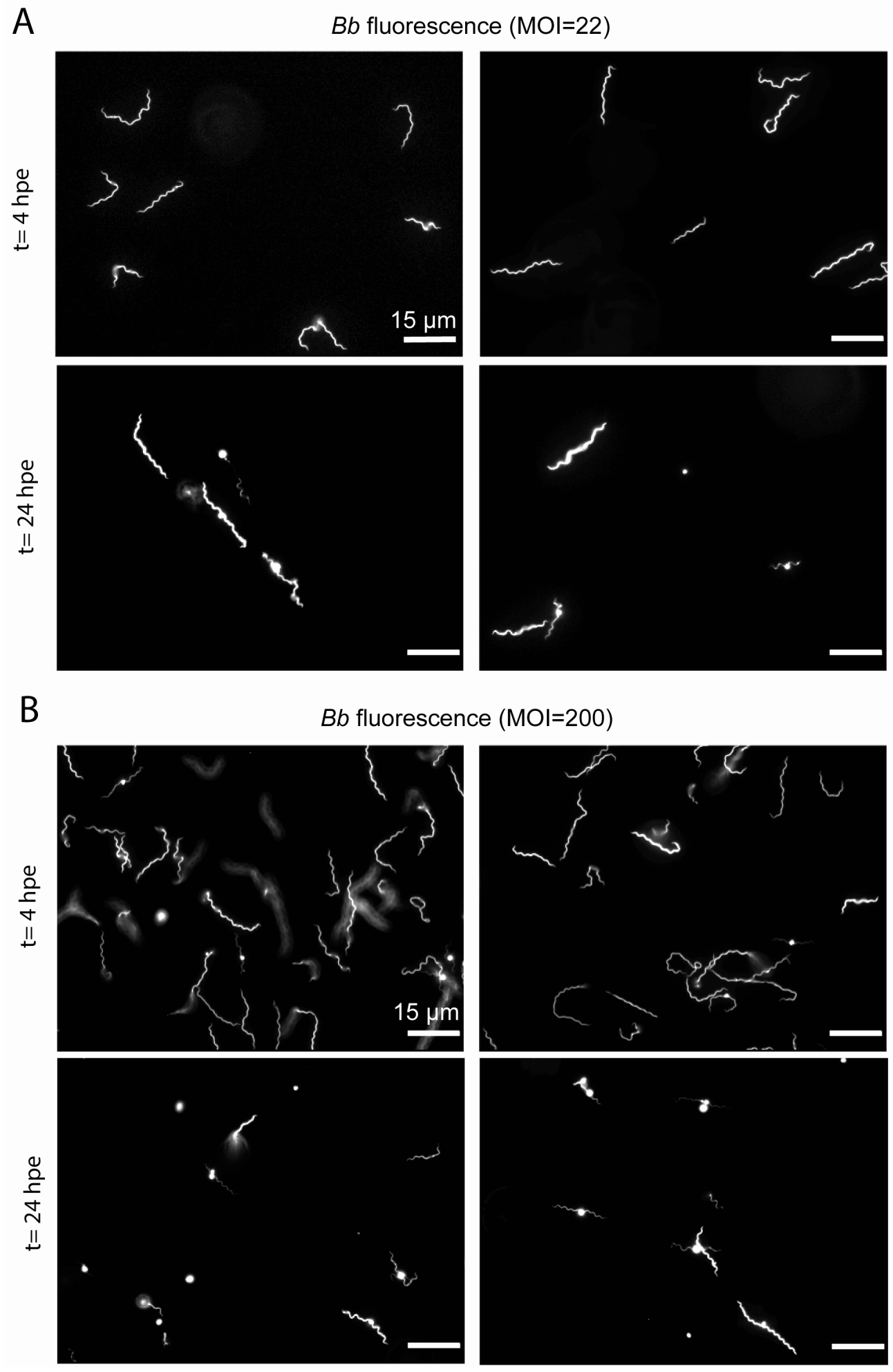

Supplemental Figure 4

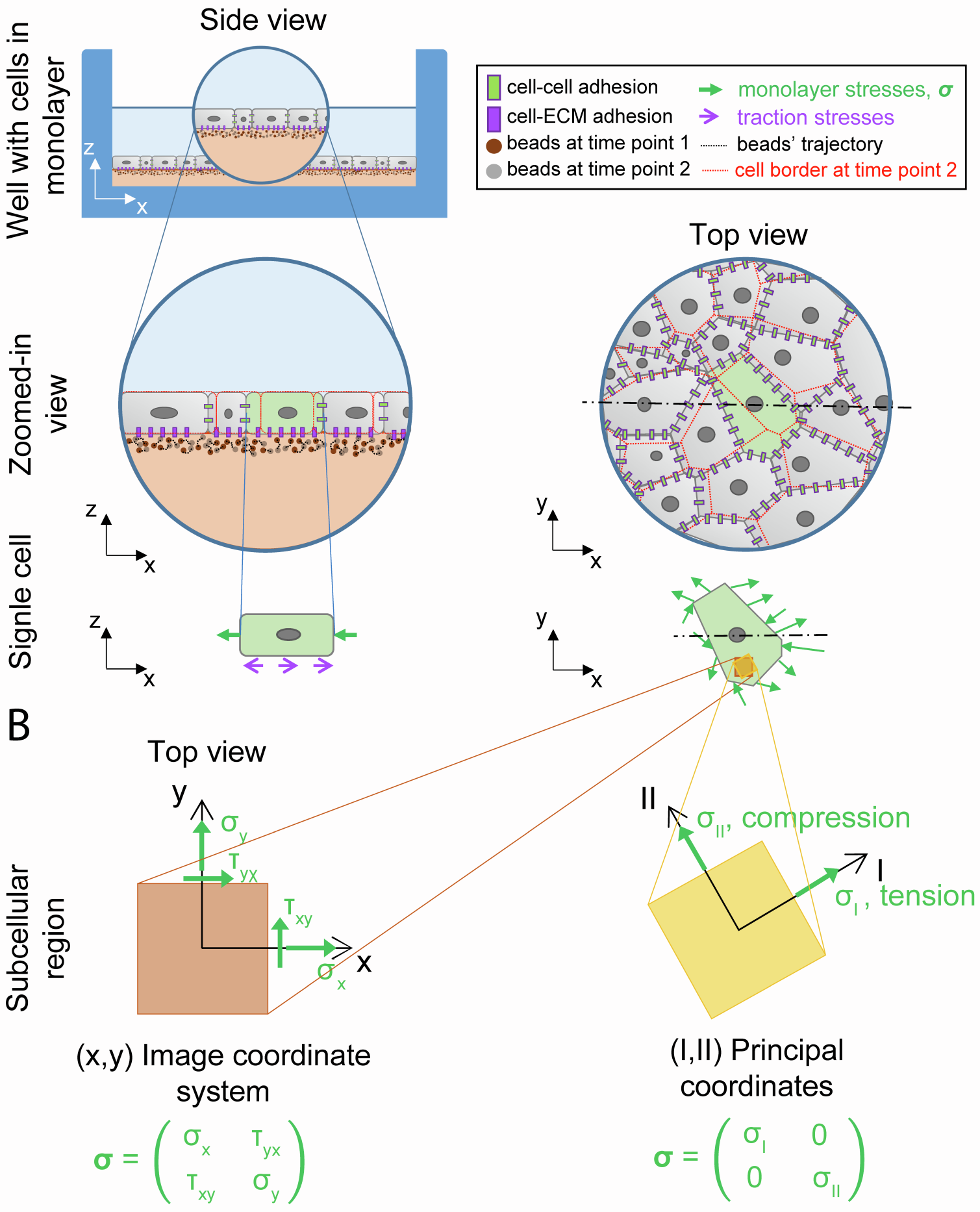

Supplemental Figure 5

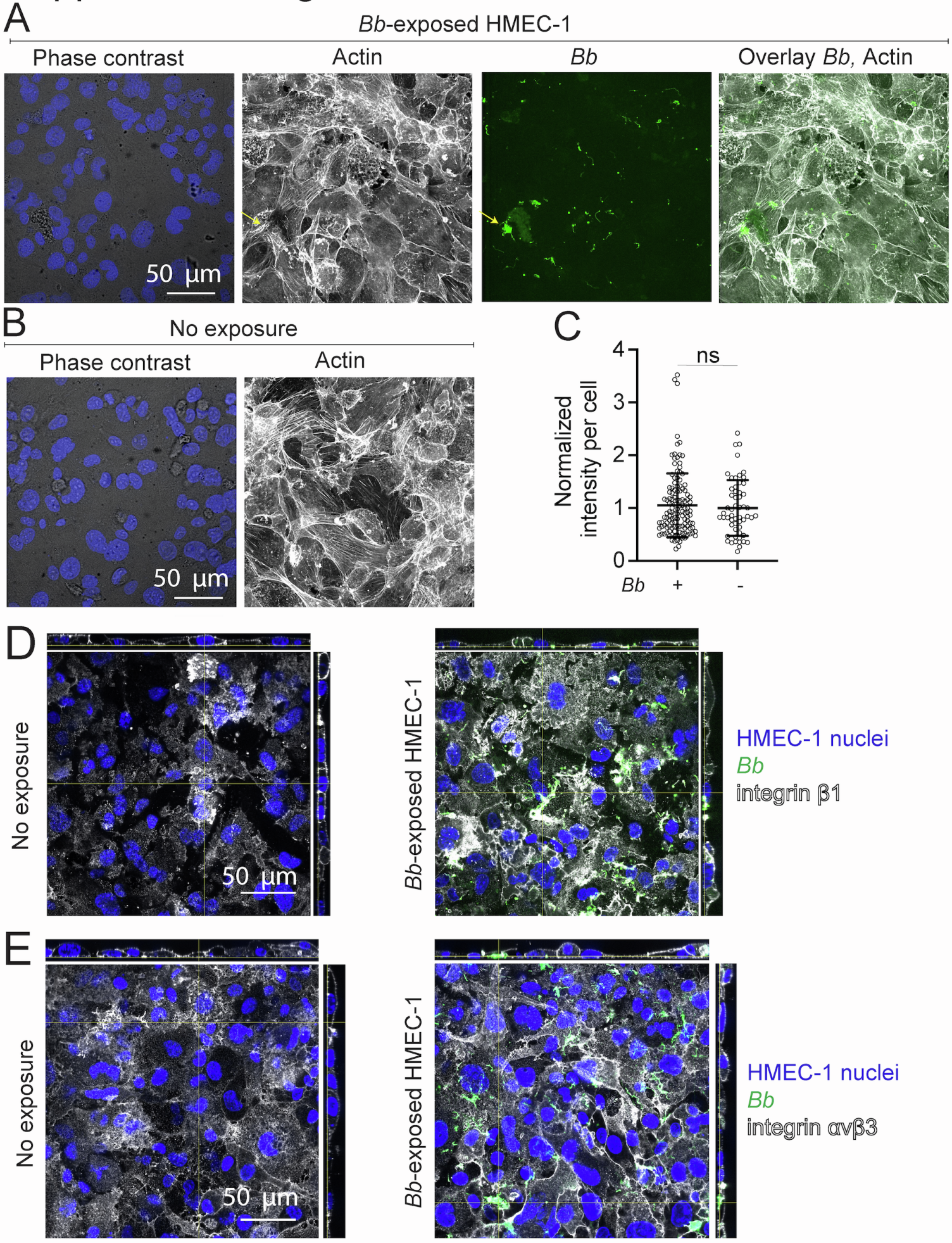

Supplemental Figure 6

A Fold increase in expression of DEGs related to NF-κB and TNF signaling during *Bb* exposure

gene	4 hpe	24 hpe	48 hpe
CXCL1	3.01	1.69	1.67
CXCL8	1.96		
CCL2	1.95	1.57	1.69
TNFAIP3	1.74		
ICAM1	1.71		
EDN1	1.63		
NFKBIA	1.61		
CXCL2	1.56		
BIRC3	1.55		
NFKB2	1.54		
RELB	1.51		

B

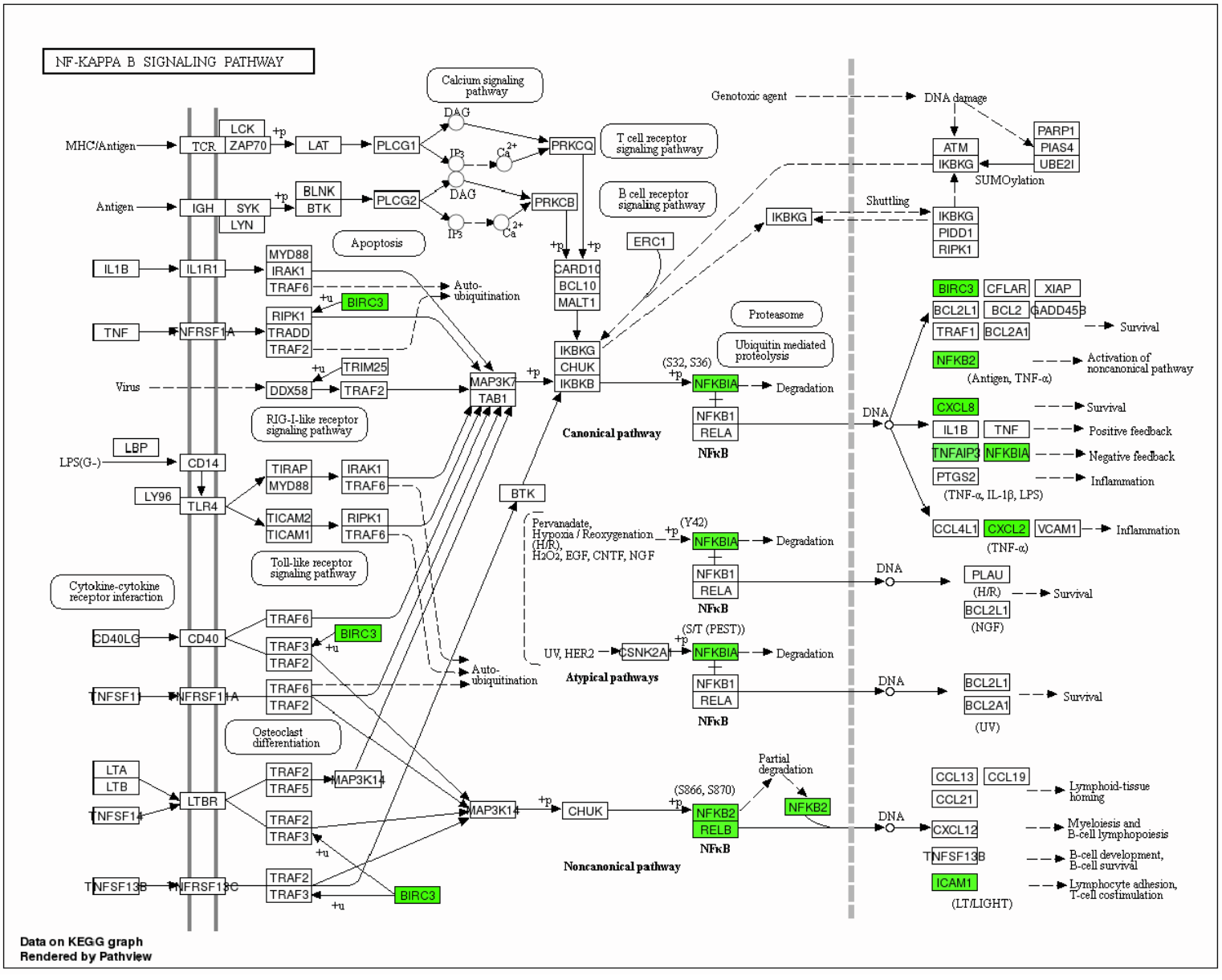

Supplemental Figure 7

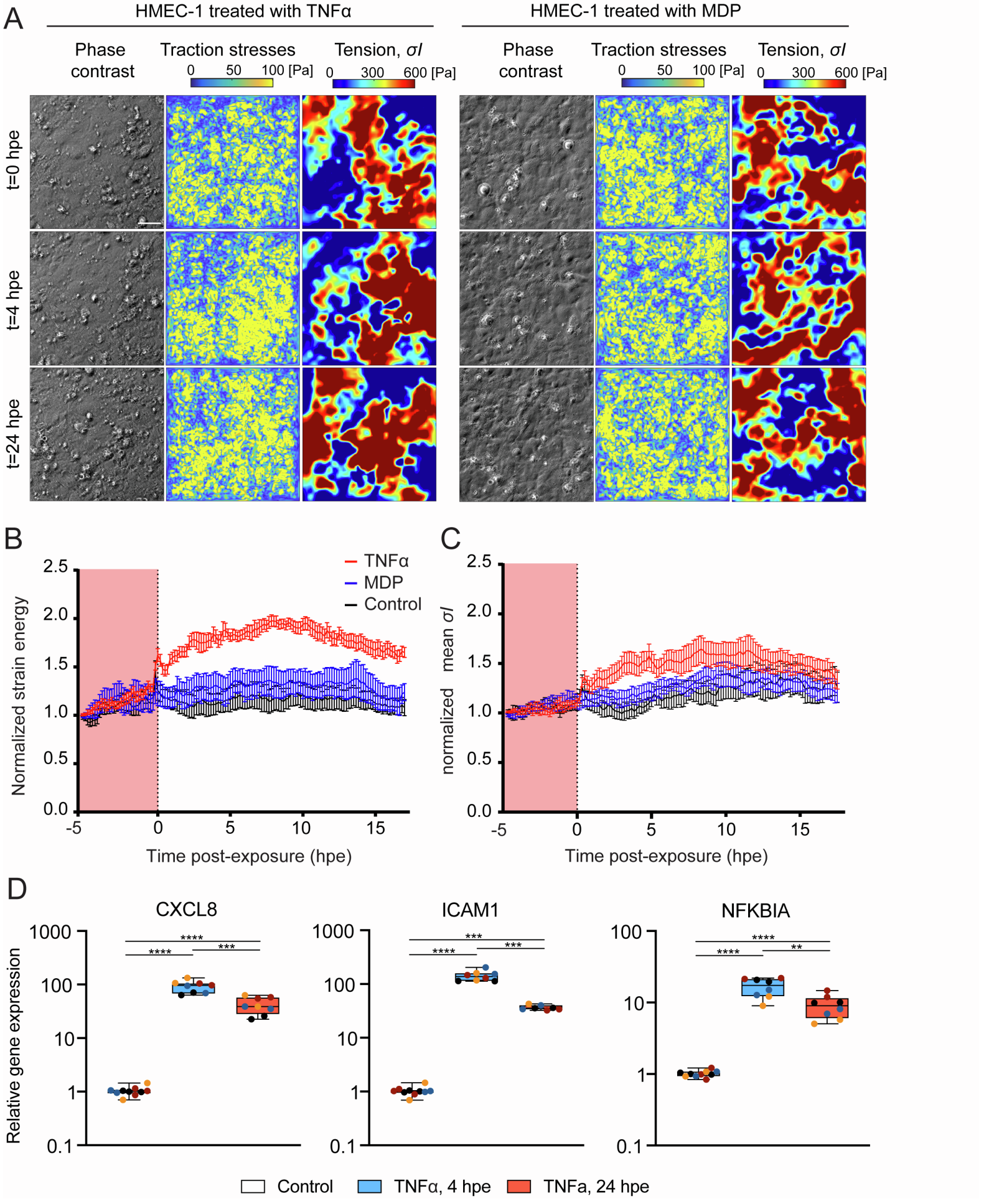

SUPPLEMENTAL FIGURE LEGENDS

Supplemental Figure 1. *Bb* can be found within HMEC-1, adhering to the apical side of HMEC-1 or transmigrated underneath the ventral side of HMEC-1. Related to Figure 1.

(**A-C**) Representative orthogonal views of fixed samples of HMEC-1 cells in monolayer exposed to *Bb* at a MOI= 0.4 at 4 hpe. Hoechst-stained host cell nuclei are shown in blue, F-actin staining with phalloidin in red (to mark host cell borders), *Bb-GFP* fluorescence in green, and extracellular bacteria immunostained with anti-*Bb* antibodies are shown in magenta. White circle in panel A indicates a bacterium internalized within HMEC-1. White circle in panel B indicates an extracellular bacterium found on the ventral side of a cell. White circle in panel C indicates an extracellular bacterium adhering on the apical side of a cell. Related to Figure 1.

Supplemental Figure 2. *Bb* viable aggregates form at late infection but single spirochetes are still present. Related to Figure 2.

(**A**) Integral of *Bb-GFP* fluorescence across the whole field of view (FOV) images for HMEC-1 in monolayer exposed to the indicated MOI of *Bb-GFP*. N=3 independent recordings were conducted (mean+/-SD). Background fluorescence was subtracted from the images. **(B)** Mean area (μm^2) occupied by *Bb-GFP* for the same recordings shown in panel A. **(C)** Representative time-lapse epifluorescence microscopy images of HMEC-1 cells in monolayer during exposure to *Bb* at a MOI = 200 and classification of bacteria into distinct classes, namely, single *Bb* (blue), network of *Bb* (magenta) and aggregates (green). Columns: phase contrast image superimposed with Hoechst-stained HMEC-1 nuclei; *Bb-GFP* fluorescence; segmented and classified bacteria. Rows: different time points post-infection (N=3 independent experiments). **(D)** Plot of the counts of classified bacterial objects versus time post-infection. Data correspond to representative recording shown in panel C and different colors correspond to each of the three different classes. (**E**) Images from representative fields of view of HMEC-1 cells in monolayer exposed for 4 h (top) or 24 h (bottom) to *Bb-GFP*. MOI=100. Columns show: brightfield image; *Bb-GFP* fluorescence; propidium iodide (PI) fluorescence; overlay of the last two channels. Yellow arrow points to *Bb* spirochetes that are not PI-positive. Yellow circles point to *Bb* aggregates that are not PI-positive. **(F)** Boxplots showing total PI fluorescence (top) and co-localization between area (μm^2) occupied by *Bb-GFP* and PI (bottom). A total of 16 images originating from four different wells (see different colors) were analyzed at 4 and 24 h post-infection (mean+/-SD, WRST: ** $p<0.01$, * $p<0.05$). Related to Figure 2.

Supplemental Figure 3. Bacterial aggregates form at late infection as a result of the high MOI, are less metabolically active than spirochetes and can revert back to spirochetes. Related to Figure 3.

(**A-B**) Epifluorescence images of supernatants of *Bb-GFP-infected* HMEC-1 cells at MOI=22 (A) or MOI=200 (B) which were collected at 4 hpe (first row) and 24 hpe (second row) and inspected by epifluorescence microscopy. For each time point and MOI two distinct fields of view are shown. Of note, at 4 hpe most of the spirochetes were motile and no morphological aberrations could be observed by dark-field or by immunofluorescence microscopy for both MOIs. At 24 hpe, some spirochetes lacked motility at both MOI=22 and MOI=200 and formed blebs. Scale bar: 15 μm. Related to Figure 3.

Supplemental Figure 4. Calculation of EC monolayer tension and compression using monolayer stress microscopy. Related to Figure 4.

(**A**) Sketch showing how a monolayer of cells in a specific well look like in a TFM experiment (top left). Underneath, a zoomed portion of the monolayer is also provided and shown on side view (left) and top view (right). Brown and grey tracer beads correspond to the location of tracer beads at two different instances of time. Their displacement is due to cells exerting traction stresses on the ECM on which the beads are embedded. As a result, the shape of the cells changes. Red dotted lines correspond to the new borders of the cells at time point 2. A zoomed-in view of a particular cell is shown on the bottom (green cell). To maintain its particular configuration, this cell is subjected to monolayer stresses (green arrows) and traction stresses (purple arrows) exerted by the ECM. (**B**) At each point of the particular cell, this results in a different stress state calculated in an arbitrary coordinate system $x-y$ (orange), with normal components σ_x, σ_y, and shear components τ_{yx}, τ_{xy}; these stresses could be rotated to a coordinated system in which the point is subjected to just normal stresses (maximum tensions (σ_I) and compressions (σ_{II})) (yellow). Note that just the stress components in the $x-y$ plane are included in this Figure. Related to Figure 4.

Supplemental Figure 5. Unexposed and *Bb*-exposed HMEC-1 cells show a different pattern of integrin localization but similar F-actin organization. Related to Figure 5.

(**A**) Representative brightfield images of cells superimposed with the Hoechst-stained nuclei image (1st column), phalloidin fluorescence to label F-actin (2nd column, maximum intensity projection), *Bb-GFP* fluorescence (3rd column, maximum intensity projection) and overlay of the last two channels (4th column) for HMEC-1 exposed to *Bb-GFP* for 8 h. (**B**) Representative brightfield images of non-exposed HMEC-1 cells superimposed with the Hoechst-stained

nuclei image (1st column) and phalloidin fluorescence to label F-actin (2nd column, maximum intensity projection). (**C**) Boxplots of mean phalloidin fluorescence intensity per cell (mean+/-SD, dots: individual cells) for HMEC-1 cells exposed with *Bb-GFP* for 8 h or uninfected cells. Mean intensity was normalized to that of cells not exposed to *Bb-GFP*. ns: non-significant change (Wilcoxon ranksum test). (**D-E**) Orthogonal views of the fields of view (FOV) shown in Figure 5 panels A and B respectively. Related to Figure 5.

Supplemental Figure 6. Genes pertaining to the NF-κB and TNF pathways show enhanced expression in HMEC-1 cells exposed to *Bb* only at 4 but not at 24 or 48 hpe. Related to Figure 6.

(**A**) Table showing the fold change of in gene expression for DEGs related to NF-κB and TNF signaling pathways in unexposed as compared to *Bb*-exposed HMEC-1 cells. NF-κB target genes NFKBIA, ICAM1 and CXCL8 are indicated in bold. (**B**) KEGG pathway map for the NF-κB signaling pathway showing in green the genes that are upregulated in *Bb*-exposed HMEC-1 at 4 hpe as compared to unexposed wells. White notes have no significance. Related to Figure 6.

Supplemental Figure 7. Exposure of ECs to TNFα but not MDP strongly upregulates expression of NF-κB target genes and increases EC force transduction for a prolonged period of time. Related to Figure 7.

(**A**) Left panels show the representative phase contrast image (1st column), EC traction stress map (2nd column, Pa) and monolayer tensile stresses σ_1 (3rd column, Pa) for HMEC-1 cells in monolayer at different time points (rows) post-addition of 10 ng/mL TNFα. TFM was performed for HMEC-1 residing on 3 kPa hydrogels. Right panels are similar, but they refer to cells exposed to 100 μg/mL MDP. (**B**) Normalized strain energy (mechanical work) imparted by cells during the course of a TFM recording (mean+/-SEM, two independent experiments and N= 12 recordings in total). Normalization was done with respect to the first value at the beginning of each recording. ECs were either exposed to vehicle control (black), or 10 ng/mL TNFα (red) or 100 μg/mL MDP (blue), and time (h) is represented relative to the time at which exposure took plate. Time prior to exposure is shaded in red. (**C**) Same as panel A but showing the normalized mean EC monolayer tensile stresses (σ_1) as a function of time post-exposure. (**D**) Expression levels of the indicated NF-κB target genes relative to *GAPDH* as obtained by RT-PCR. N=3 independent experiments were performed. Three conditions were tested, namely, ECs exposed to vehicle control, or to 10 ng/mL TNFα for 4 h (blue) or for 24 h (red). From left to right normalized expression of the following genes is shown: CXCL8, ICAM1,

NFKBIA. Boxplots show the mean, 25th and 75th quartiles, different colors refer to replicates from independent experiments, *: p<0.05, **: p<0.01, ***: p<0.001, ****: p<0.0001 (Wilcoxon ranksum test run for each condition's distribution with respect to control). See also Figure 7.